

See discussions, stats, and author profiles for this publication at: <https://www.researchgate.net/publication/242338509>

# A revised Michel-Lévy interference colour chart based on first-principles calculations

Article in *European Journal of Mineralogy* · February 2013

DOI: 10.1127/0935-1221/2013/0025-2252

---

CITATIONS

208

---

READS

27,721

1 author:



[Bjørn Eske Sørensen](#)

Norwegian University of Science and Technology

83 PUBLICATIONS 878 CITATIONS

SEE PROFILE

# A revised Michel-Lévy interference colour chart based on first-principles calculations

BJØRN ESKE SØRENSEN\*

Department of Geology and Mineral Resources Engineering, Norwegian University of Technology and Science (NTNU), Sem Seelandsveg 1, 7491 Trondheim, Norway

\*Corresponding author, e-mail: Bjorn.sorensen@ntnu.no

**Abstract:** Two revisions of the original Michel-Lévy interference colour chart are presented, and discussed here. Compared to older charts these give a more precise match to the actual observations in the modern optical microscope. As an example, interference colour transitions on wedge shaped olivine grain boundaries toward epoxy match accurately the interference colour in the new charts. The differences in the colour between older charts and the new are most pronounced in the second order, where the saturated green is now replaced by greenish white and turquoise. In addition, the pinks are shown to cover a larger range than previously thought. The revised charts make it easier to determine interference colour and order, and hence also to determine the birefringence of the common silicate minerals. Because of the first-principle origin of the charts it is easy to adjust the charts for different types of optics and illumination. Also the improved understanding of interference colour opens up new possibilities in image analysis of transmitted-light images involving interference colour.

**Key-words:** optical microscopy, interference colour chart, Michel-Lévy, interference colour, optical mineralogy, birefringence, optical crystallography.

## 1. Introduction

Students are commonly confused when first introduced to the phenomena of interference colours and determination of birefringence. Today most optical microscopes are only equipped with  $\frac{1}{4}$ -lambda and 1-lambda plates and hence rely on different versions of the Michel-Lévy interference colour charts. This is commonly a big challenge not helped by the mismatch between observed interference colours and those displayed in the charts.

The aim of this study is to produce a birefringence colour chart that presents the interference colours as they are observed in the microscope by using the original light interference equations to produce the spectral colours, and then transform them into human vision and device colours that can be viewed on a computer screen.

## 2. Methodology

The interference colour charts were calculated in MATLAB using the relations between light transmission and wavelengths. For a given wavelength ( $\lambda$ ) in nm the degree of transmission  $L$ , can be calculated according to the equation (e.g., Bloss, 1999):

$$L = \cos^2 \varphi - \sin^2(\tau - \varphi) \sin^2(\tau) \sin^2\left(\frac{180^\circ \Gamma}{\lambda}\right) \quad (1)$$

where  $\varphi$  is the angle between vibration directions of the polarizer and analyzer,  $\tau$ , the angle between the polarizer's privileged direction and the crystal's closest privileged direction,  $\lambda$  the wavelength of light and  $\Gamma$  ( $\Gamma = d \times (n\gamma - n\alpha)$ ), the retardation or path difference produced during passage of light through the crystal.

When the angle between the analyser and polarizer ( $\varphi$ ) is  $90^\circ$  Equation (1) reduces to:

$$L(\Gamma, \lambda) = \sin^2\left(\frac{180^\circ \Gamma}{\lambda}\right) \quad (2)$$

Applying Equation (2) to wavelengths in the visible spectrum (360–830 nm) and possible retardations produces a spectral transmission matrix ( $I_\lambda$ ):

$$I_\lambda = \begin{bmatrix} L(\Gamma_1, 360 \text{ nm}) & \cdots & L(\Gamma_n, 360 \text{ nm}) \\ \vdots & \ddots & \vdots \\ L(\Gamma_1, 830 \text{ nm}) & \cdots & L(\Gamma_n, 830 \text{ nm}) \end{bmatrix} \quad (3)$$

This spectral colour matrix cannot be displayed on any print or screen device and needs to go through a two-step conversion process:

(1) Since the purpose is to produce a chart representative of what we observe with the human eye in the optical microscope, the first step is to recalculate spectral

colour to human vision colour. The CIE1931 colour matching functions (CIE, 1931) in tabulated form (CVRL database) was used for this conversion (Fig. 1, Equation (4)):

$$L_{XYZ} = \begin{bmatrix} X \\ Y \\ Z \end{bmatrix} = \begin{bmatrix} \vec{r}_\lambda \\ \vec{g}_\lambda \\ \vec{b}_\lambda \end{bmatrix} I_\lambda \quad (4)$$

where  $I_\lambda$  is the spectral colour matrix for all retardations,  $\vec{r}_\lambda$ ,  $\vec{g}_\lambda$  and  $\vec{b}_\lambda$  the sensitivity functions for red, green and blue respectively (Fig. 2) and  $X$ ,  $Y$  and  $Z$  the human vision colour coordinates.

(2) Digital devices do not display directly human vision colour and hence transformation to RGB was needed to display the results on the computer screen. For the present case Adobe RGB was used, but there are several other RGB colour models available. The transformation is a two step process. First a linear transformation is performed (*e.g.*, Pascale, 2003):

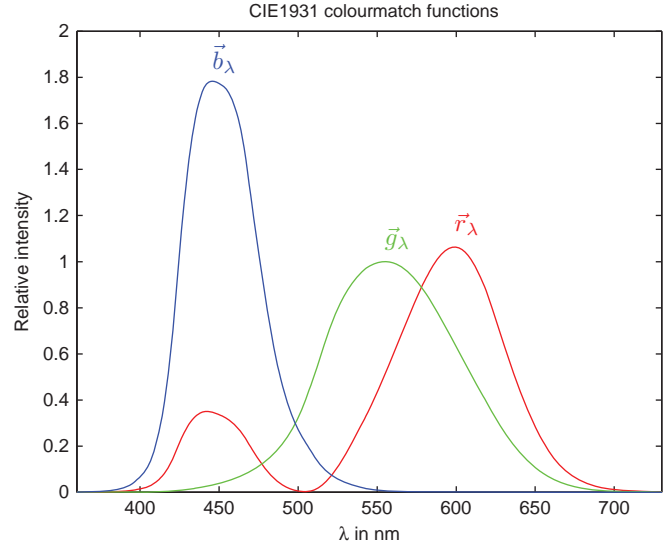


Fig. 1. Colour sensitivity functions for red, green and blue, after CIE (1931). Used to calculate CIEXYZ human vision colour from spectral colour.

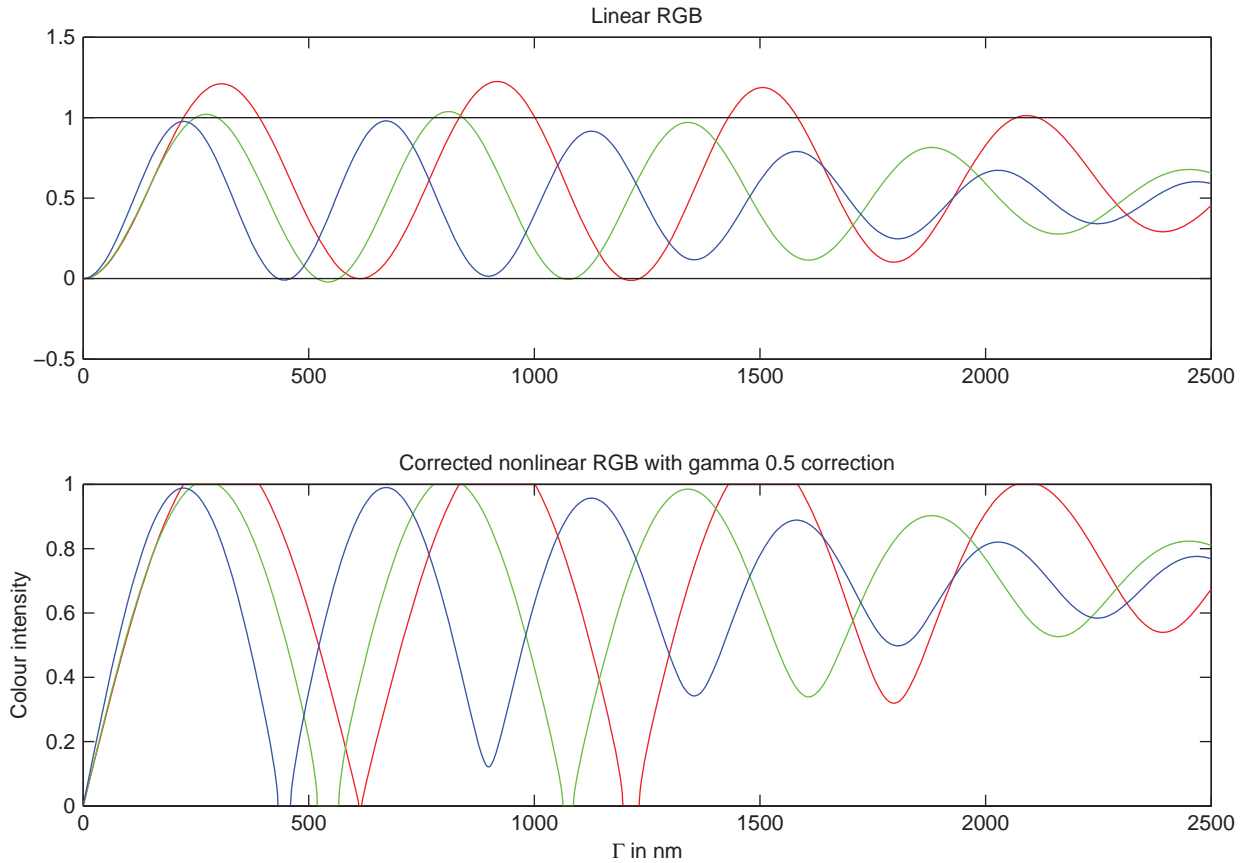


Fig. 2. Upper part: values of red (red line), green (green line) and red linear RGB values after transformation from CIEXYZ. Lower part shows the nonlinear final colours after gamma correction of 0.5 and clipping of values above 1 and below 0.

$$\text{RGB}_{\text{linear}} = \begin{bmatrix} R \\ G \\ B \end{bmatrix} = \text{MRGB} * \begin{bmatrix} X \\ Y \\ Z \end{bmatrix} \quad (5)$$

For Adobe RGB MRGB equals (Pascale, 2003):

$$\text{MRGB} = \begin{bmatrix} 2.04414 & -0.5649 & -0.3447 \\ -0.9693 & 1.8760 & 0.0416 \\ 0.0134 & -0.1184 & 1.0154 \end{bmatrix} \quad (6)$$

The linear RGB values exceed the allowed range of values between 0 and 1 (Fig. 2). This is especially pronounced for the red values. To preserve the intensity values of first order white a simple clipping adjustment was applied, such that values above 1 were set to 1 and values below 0 were set to 0. This step is important because the clipping of values above 1 is the only way to get the first-order white as white and not grey as seen in many charts. A gamma correction was used to transfer the linear RGB to nonlinear R'G'B' values which display correctly on e.g. computer screens. A typical gamma value for thin section imaging is about 0.5 and gives an image on the screen that matches the colour contrast seen by the eye. The built-in ‘‘imadjust’’ function in MATLAB was used for this.

### 3. Results and discussion

Results demonstrate that a Michel-Lévy chart can easily be calculated using programming and published colour

transformation functions. Because of the wide gamut range of the interference colours, a colour clipping of the red values is necessary. Here I demonstrate that the chart gives good representation of the normal interference colours observed in the optical microscope.

Two types of charts are presented here: (1) revision of the original Michel-Lévy charts (Fig. 3) and (2) Raith-Sørensen chart, representing interference colour directly as a function of birefringence and thin-section thickness (Fig. 4).

The calculated chart matches thin section observations of natural silicates well. Figure 5 illustrates this by using three common silicates, olivine, talc and quartz as examples. An olivine grain mounted in epoxy shows second-order yellow interference colour in the middle (Fig. 5b). The olivine grain boundary has a wedge-shaped grain-boundary, meaning that the grain is thinner towards the rim. This also causes the interference colours to decrease, because the grain is mounted in isotropic epoxy and interference colour is a function of path difference, which is birefringence multiplied by thickness. In this way the grain boundary represents a small part of the interference colour range from path difference 0 up to the second-order yellow displayed in the middle of the grain. An insert of the calculated chart shows that there is good agreement between the calculated and observed interference colours. By using the 1-lambda compensator plate the interference colours can be shifted order up or down by approximately one order (Fig. 5a, c). Here, inserts of the calculated chart show good agreement with the observed interference colours. This confirms that the calculated chart represents interference colours up to the

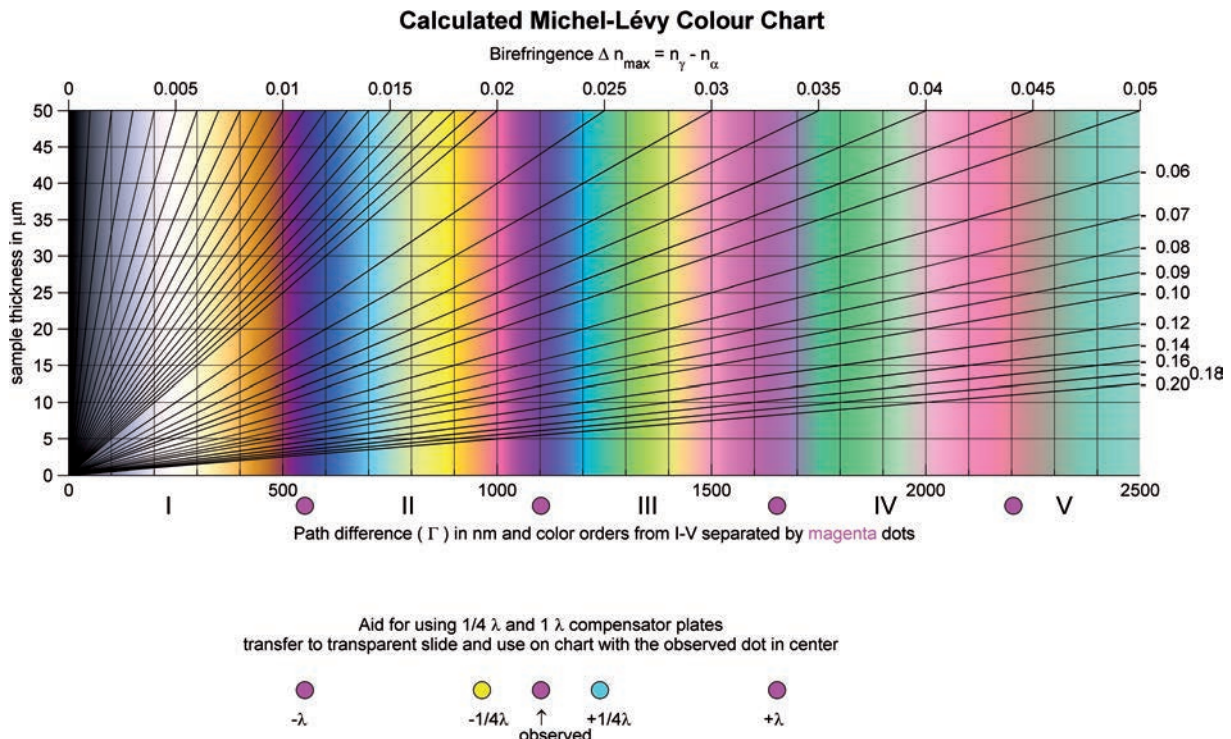


Fig. 3. Michel-Lévy chart. Markers for use of 1-lambda and 1/4-lambda plates added.

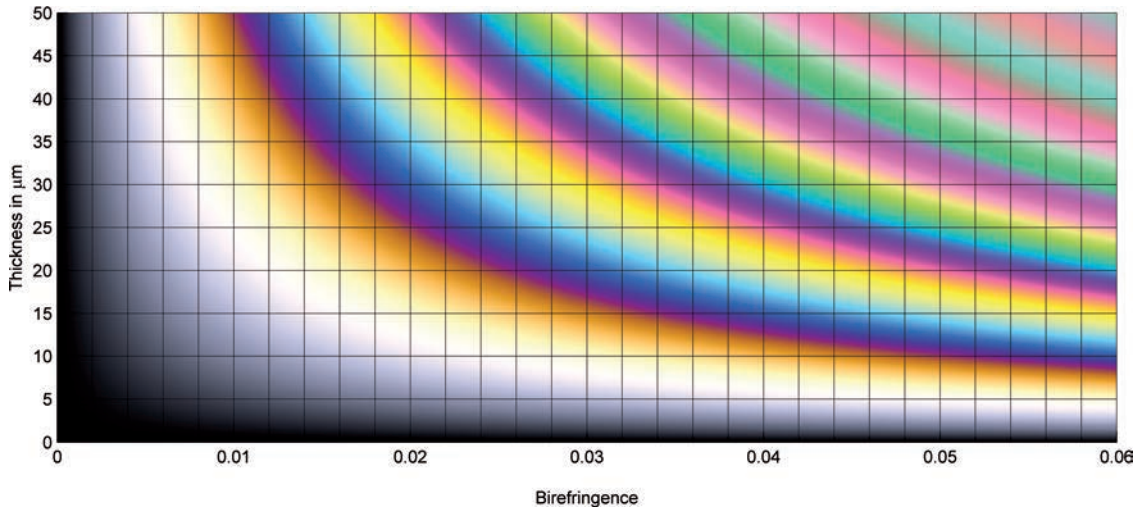


Fig. 4. Raith–Sørensen chart. Direct representation of interference colour as a function of birefringence and sample thickness.

third-order green. This is also the case for other common rock-forming minerals. For example, talc, with birefringence of 0.0370–0.0500, typically showing third-order green to pink third-order maximum interference colours is included. First the third-order green is identified in the chart (Fig. 5e). By inserting the lambda plate with the grain in addition orientation (slow on slow) the fourth-order green is obtained (Fig. 5f). Again the observed colour matches the calculated colour. By rotating the grain 90° the grain is in subtraction position and with the lambda plate inserted the colour reduces by approximately one order, at the boundary between second-order turquoise blue and yellow (Fig. 5d). Again the calculated and observed interference colours agree (Fig. 5d, g). Quartz has low variation in birefringence with wavelength and hence displays normal birefringence colours, which should agree with the calculated values. A comparison with images of quartz grains in immersion oil from Dyar & Gunter (2007) shows agreement between observed and calculated colours for the full colour range (Fig. 5h). Similarly the calculated chart matches the colours observed in a quartz wedge (Fig. 5i), shown in Figure 16.19c of Dyar & Gunter (2007). From the above observations it is concluded that the calculated chart perfectly reproduces the interference colours displayed by common silicates.

The calculated chart is different from other commonly used charts, not only by differences in colour but also in the positioning of the retardation scale in relation to the interference colours. Only a brief comparison is provided here (Fig. 6), and the interested reader is referred to the more extensive review by Delly (2003).

The chart that differs most from the new calculated chart is the chart first published by Zeiss in 1963 (Gahm, 1963), which is also used in optical mineralogy books such as Nesse (2003) (Fig. 6a). First, the colours are quite different, especially in the second order, where the old charts display a large portion of saturated green in the lower part of the second order (Fig. 6a). Compared with the new chart and thin section and quartz wedge observations, this should

be more blue and turquoise blue, grading through whitish blue-green into yellow (Fig. 5 and 6d). However, when it comes to the retardation scale it seems that there is good agreement, with the orders being separated by pink colours, *i.e.* boundary a first, second and third order pink (compare Fig. 6a, d).

Another commonly used chart is the one by Leitz (1985), also used in Bloss (1999) (Fig. 6b). When it comes to colour this chart is closer to the calculated chart, though there still is too much green in the second order. Another marked difference is that the boundaries between the interference colour orders are placed to high in the Leitz chart. The boundary should be at the pink colours, as in the calculated chart, as it can be checked by stacking multiple 1-lambda plates with 551 nm retardation on top of each other.

The chart which looks most similar to the calculated chart here, is the one presented in Figure 16.27 of Dyar & Gunter (2007). This chart was produced by photographing a quartz wedge under crossed polars and adding the retardation scale later, using several 1-lambda compensator plates, to find the boundaries between the interference colour orders. The only difference between the calculated colours and the Dyar & Gunter (2007) chart is that the Dyar & Gunter (2007) display less saturated colours, compared to the calculated chart (compare Fig. 6c, d). When it comes to retardation scale the Dyar & Gunter (2007) chart places the order boundaries lower in the pink colours than the calculated chart (compare Fig. 6c, d). In practical sense this means that the Dyar & Gunter (2007) chart can be used to determine the interference colour and order, though some small deviation in the retardation and hence birefringence would be expected. The new calculated chart is more accurate when it comes to determination of retardation and birefringence, and furthermore the calculation method has the advantage that interference colour data can be represented in any form, for example, as in the Raith–Sørensen chart (Fig. 4) where interference colour, birefringence and sample thickness are directly related.

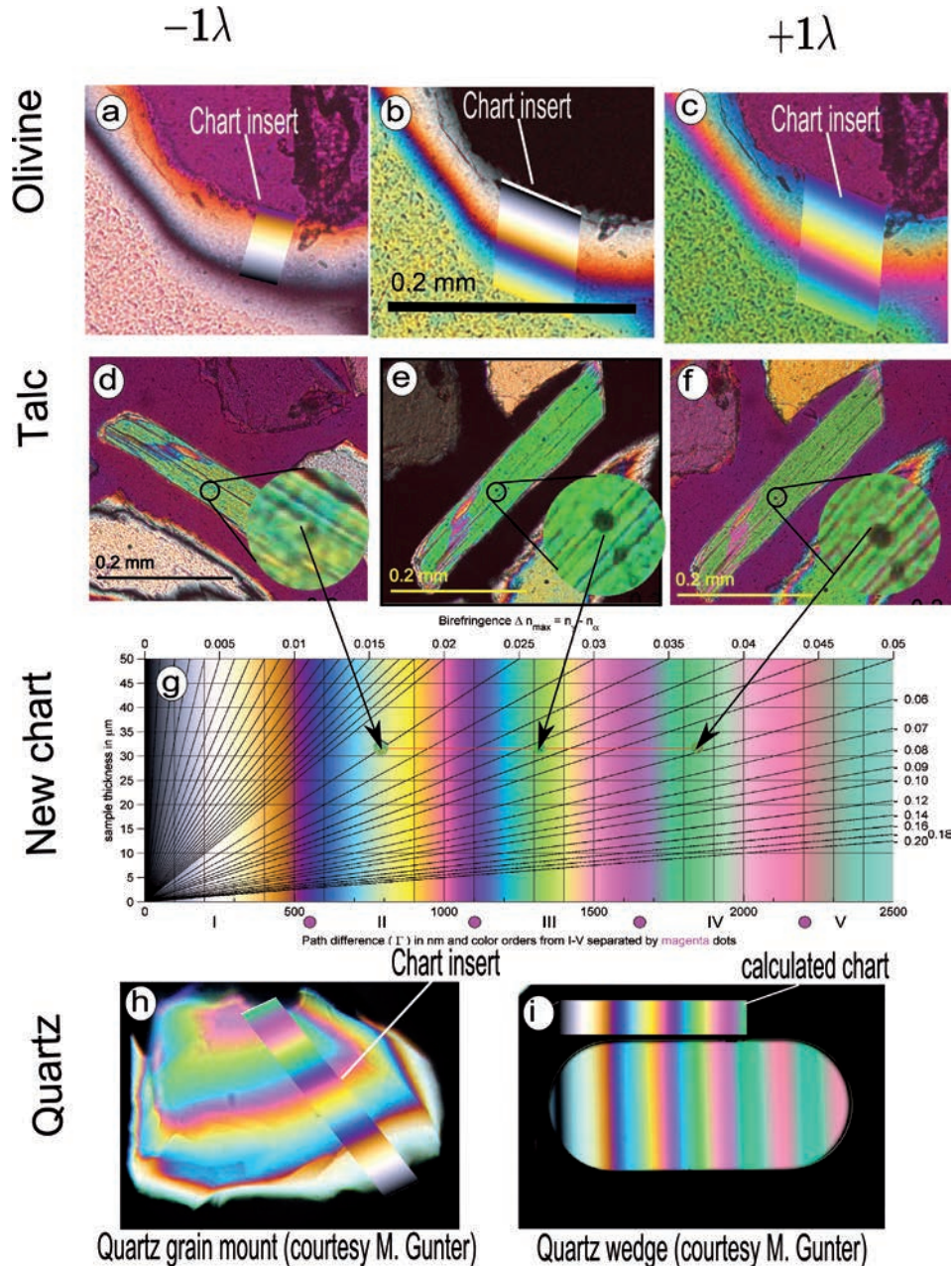


Fig. 5. Verification of the calculated Michel-Lévy chart by optical microscope observations. (a–c) are images of olivine grain with a wedge-shaped grain boundary toward epoxy, giving a rim-ward thinning of the grain and hence also decreasing interference colour. Insert of the calculated chart for comparison with the observed colour. (a) Interference colour is observed with the 1-lambda plate in subtraction orientation. (b) Interference colour observed without compensator plates. (c) Interference colour is observed with 1-lambda compensator plate in addition orientation. (d–g) Comparison of the chart (g) with a talc grain displaying third-order turquoise colour without compensator plate (e), mid second-order turquoise in 1-lambda subtraction (d) and fourth-order green in 1-lambda addition. This agrees well with the calculated chart (g). (h–i) are comparisons for quartz in immersion oil (h) and quartz wedge (i).

In conclusion, the calculated chart gives an accurate representation of the interference colours observed in the petrographic microscope, and also gives a direct relation between the colour and the retardation. If the retardation of compensator plates are known then these can be used to refine the retardation and hence also birefringence determination. The calculated chart represents a significant improvement compared to older charts, not only by giving

a more precise match with the interference colour, but also by an accurate retardation scale. The new charts are designed primarily as an improved teaching aid for inexperienced microscopists to help with the determination of birefringence. In addition, the simple calculation method giving an accurate colour representation opens up the possibility to improve image analysis of birefringent minerals in transmitted light under crossed polars.

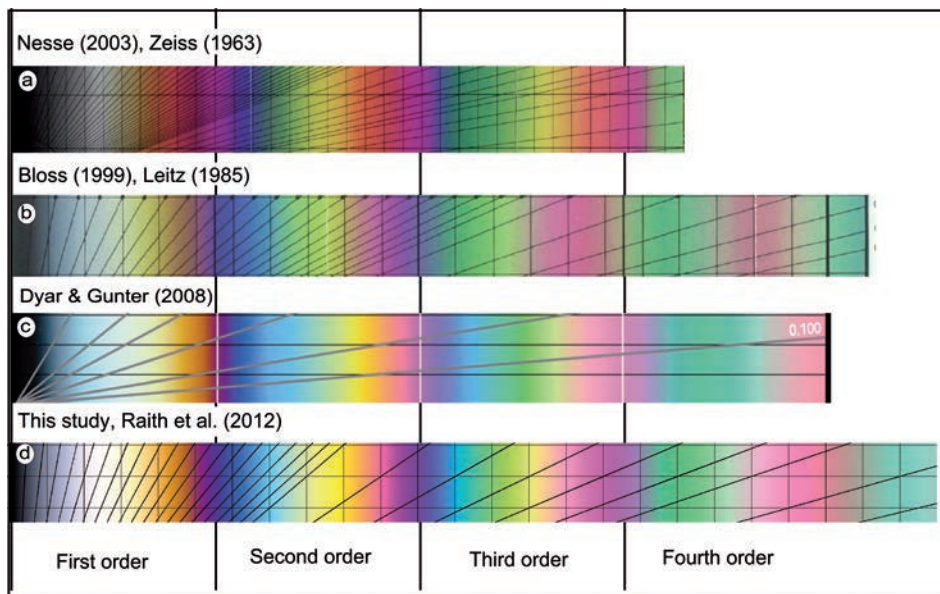


Fig. 6. Comparison of the new chart with other available and commonly used charts. (a) The Zeiss chart, also used in Nesse (2003). (b) The Leitz chart, also used by Bloss (1999). (c) The quartz-wedge chart by Dyar & Gunter (2007). (d) This study, the calculated chart, now used by Raith *et al.* (2012).

**Acknowledgements:** Professor M. Raith is deeply acknowledged for his interesting discussion and creative suggestions to the manuscript. He did important testing of my charts by comparisons with my simulated colour. His criticism greatly improved the match of the charts, ending up with their final appearance as presented here. Professor A.G. Krill and Suzanne McEnroe helped to improve the readability of the manuscript. Comments by M. Gunter aided the full documentation of the chart by useful suggestions and by making his figures available to me.

## References

- Bloss, F.D. (1999): Optical crystallography. Mineralogical Society of America, Washington, DC.
- CIE (1931): Commission internationale de l'Éclairage proceedings, 1931. Cambridge University Press, Cambridge.
- CVRL database: <http://cvrl.ioo.ucl.ac.uk/index.htm> (August 2011).
- Delly, J.G. (2003): The Michel-Lévy interference color chart – microscopy's magical color key: <http://www.modernmicroscopy.com/main.asp?article=15&print=true&pix=true>
- Dyar, M.D. & Gunter, M.E. (2007): Mineralogy and Optical Mineralogy. Mineralogical Society of America, Chantilly, VA, 706 p.
- Gahm, J. (1963): The interference color chart according to Michel-Lévy. Reprint from Zeiss Werkzeitschrift No. 46. Carl Zeiss, Oberkochen.
- MATLAB ver R 2009b. Mathworks.inc, Natick, MA.
- Nesse, W. (2003): Introduction to Optical Mineralogy. 3<sup>rd</sup> Edition, Oxford University Press, New York.
- Pascale, D., 2003, A review of RGB color spaces . . . from  $xyY$  to  $R'G'B'$ : <http://www.babelcolor.com/download/A%20review%20of%20RGB%20color%20spaces.pdf> (August 2011)
- Raith, M.M., Raase, P., Reinhardt, J. (2012): Guide to Thin Section Microscopy. 2<sup>nd</sup> Edition, 127 p. ISBN 978-3-00-037671-9.

*Received 11 April 2012*

*Modified version received 20 June 2012*

*Accepted 13 August 2012*